research papers

Diffusion in solids studied by nuclear resonant X-ray and neutron scattering†

Martin Kaisermayr,[a]* Bogdan Sepiol,[a] Jerome Combet,[b]‡ Rudolf Rüffer,[c] Catherine Pappas[d] and Gero Vogl[a]

[a]*Institut für Materialphysik der Universität Wien, A-1090 Wien, Austria,* [b]*Institut Laue-Langevin, F-38042 Grenoble, France,* [c]*European Synchrotron Radiation Facility, F-38043 Grenoble, France,* and [d]*Hahn-Meitner Institut, D-14109 Berlin, Germany.* E-mail: kaiserm@ap.univie.ac.at

Nuclear resonant scattering of synchrotron radiation and quasielastic neutron scattering allow the measurement of frequencies, directions and lengths of jumps of diffusing atoms. Both methods have been successfully applied to diffusion in solids. Synergies and respective advantages of these two techniques as well as recent developments are discussed on the basis of an example: diffusion in intermetallic alloys.

Keywords: diffusion; QNS; NRS.

1. Introduction

Intermetallic alloys are increasingly used for high-temperature applications owing to their corrosion stability and strength. Their extraordinary properties at elevated temperatures are strongly connected to self-diffusion, *i.e.* diffusion of the constituents themselves. Knowledge of the kinetics on the atomistic scale in these systems may permit crucial processes to be controlled, *e.g.* different stages of precipitation, and so to tailor the macroscopic features of these materials. However, even in intermetallics with structures as simple as the CsCl structure, the mechanism of self-diffusion is not yet fully understood. This is due to the complex interplay between diffusion and local order which occurs in these systems where the diffusive jump is directly related to the creation or destruction of a point defect (Mehrer, 1996).

Quasielastic neutron scattering (QNS) and nuclear resonant scattering of synchrotron radiation (NRS) can essentially contribute to the investigation of the diffusion process in intermetallic compounds since they both allow the observation of diffusion on the atomistic scale by measuring the frequency, distance and direction of the atomic jump (Hempelmann, 2000; Vogl & Feldwisch, 1998; Sepiol *et al.*, 1996).

2. Diffusion studies with QNS

Quasielastic neutron scattering allows one to retrieve information on the motion of diffusing atoms from the quasielastic broadening of the elastic incoherent§ line.

For vacancy diffusion in intermetallic alloys, *i.e.* diffusion between sites of different sublattices, the quasielastic line is a sum of N Lorentzians, where N is the number of different sublattices visited by the diffusing atom. Both widths and relative weights of the N Lorentzians depend on the scattering vector $\mathbf{Q}$. The line widths Γ are proportional to the eigenvalues of a matrix $\mathbf{A}$ (Rowe *et al.*, 1971; Kutner & Sosnowska, 1977; Randl *et al.*, 1994) containing the scattering vector, the jump vectors and the residence times on the different sublattices,

$$A_{ij} = \frac{1}{n_{ji}\tau_{ij}} \sum_{k=1}^{N} \exp(-i\,\mathbf{Q}\mathbf{l}_{ij}^k) - \delta_{ij} \sum_{k=1}^{N} \frac{1}{\tau_{ik}}, \qquad (1)$$

where $\mathbf{l}_{ij}^k$ denotes the kth jump vector leading from a site on sublattice i to a site on sublattice j, τ_{ij} is the average residence time of an atom on sublattice i before jumping to sublattice j, and n_{ji} is the number of target sites on the ith sublattice which are accessible from sublattice j.

In the following we discuss experiments using the two neutron scattering techniques which allow one to determine the jump vectors of atoms diffusing on their lattices: high-resolution backscattering spectrometry and neutron spin–echo spectrometry.

2.1. Backscattering

Diffusivities in intermetallic alloys rarely exceed $D = 10^{-12}$ m^2 s^{-1} (Mehrer, 1996) which corresponds to mean residence times of some nanoseconds. Hence, an energy resolution better than μeV is required. Backscattering spectrometers like IN10 or IN16 at the ILL provide resolution functions with a typical half-width of 1 μeV. Owing to high flux and stability the resolution functions as well as the quasielastic spectra can be measured with high accuracy, so that line broadenings of 0.1 μeV can still be resolved.

Thus, it has not only been possible to determine the diffusive jump in systems with fast diffusion like NiSb (Vogl *et al.*, 1993) or Ni$_3$Sb (Vogl *et al.*, 1996) but also in the class of $B2$ alloys where diffusion is comparably slow.

The $B2$ structure (= CsCl structure) consists of two simple cubic lattices where the sites of the first sublattice are in the centre of the unit cell of the second one and *vice versa* (see inset in Fig. 1). Hence,
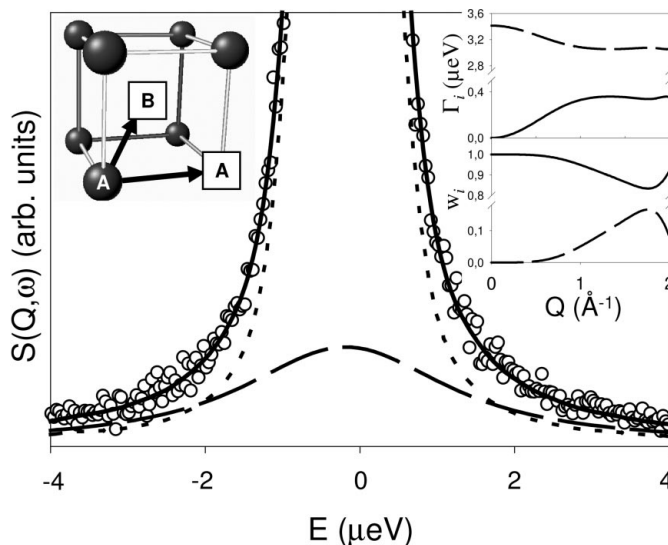

Figure 1
Quasielastic spectrum obtained from an Ni$_{51}$Ga$_{49}$ single crystal at 1403 K and $Q = 1.6$ Å^{-1} (Kaisermayr *et al.*, 2000). The dashed and dotted lines represent the two Lorentzians. First inset: $B2$ unit cell. The arrows represent a jump of an A atom to an NN and an NNN site on the B and A lattice, respectively. Second inset: Q-dependence of the widths Γ_i and weights w_i of the two Lorentzians as calculated for Ni diffusion *via* NN jumps with a ratio of residence times $\tau_{Ga}/\tau_{Ni} = 0.12$.

---

the diffusing atoms have to choose between two energetically unfavourable options: jumps to nearest-neighbour (NN) sites, which belong to the 'wrong' sublattice (anti-sites), or more distant jumps to next-nearest-neighbour (NNN) sites on the regular sublattice.

Two $B2$ alloys which were recently studied with QNS are NiGa (Kaisermayr *et al.*, 2000) and CoGa (Kaisermayr, Combet, Ipser *et al.*, 2001). Fig. 1 shows a quasielastic spectrum as obtained from an NiGa single crystal in an orientation as defined by Kaisermayr *et al.* (2000). The best fit to the spectra corresponding to different $\mathbf{Q}$ vectors is obtained with a model based on NN jumps. The same jump vector was found for Co diffusion in CoGa. The inset in Fig. 2 shows, for a particular orientation of a CoGa single crystal as specified by Kaisermayr, Combet, Ipser *et al.* (2001), the $\mathbf{Q}$-dependence of the narrower of the two Lorentzians as fitted to the experimental spectra and as calculated for an NN-jump model.

For both alloys, a comparably long residence time on the anti-sites was found which corresponds to high defect concentrations of the order of several percent.

In addition, QNS yields information on the correlation of subsequent jumps. The correlation factor relates the long-range diffusion to the frequencies of individual jumps. It can be determined by a comparison of corresponding linewidths measured at Q values corresponding to interatomic distances and linewidths in the limit of small Q (hydrodynamic limit). In both alloys, NiGa and CoGa, a correlation factor close to unity has been found (Kaisermayr, Combet, Sepiol & Vogl, 2001), thus indicating a weak correlation of subsequent jumps. Hence, the atoms and the vacancies move in a rather stochastic way, which is astonishing insofar as a vacancy that moves stochastically through the sample *via* NN jumps leaves a path of disorder behind so that the vacancies (and therewith the atoms) are expected to perform some sort of correlated movement. Apparently, this effect is strongly reduced if there is a certain degree of disorder present in the sample.

2.2. Neutron spin–echo

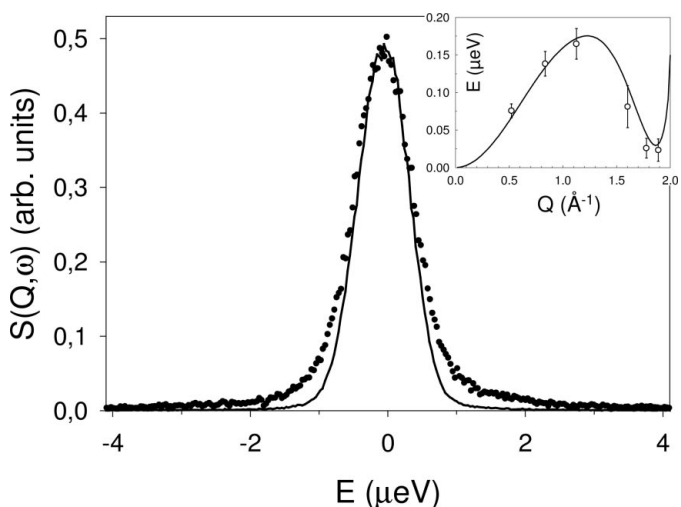Today's world-class spectrometers have practically reached the theoretical limit that can be expected from this technique in terms of energy resolution. This is a considerable restraint for future research in the field of diffusion in solids because the presently accessible diffusivities limit the range of systems that can be investigated to systems with low to intermediate order which, in addition, have to be studied at very high temperatures, often close to the melting point.

Owing to instrumental developments in the field of neutron spin–echo spectroscopy (NSE) it was recently possible to apply this technique to diffusion in solids (Kaisermayr, Combet, Sepiol & Vogl, 2001), and therewith to achieve a considerably higher resolution which will open new classes of alloys to direct diffusion studies.

An important advantage of this technique, besides its outstandingly high resolution, is its ability to measure directly in the *time domain* and therefore to give an immediate picture of the different time scales involved in the diffusion process. Every Lorentzian in the energy domain (as measured on the backscattering spectrometer) corresponds to an exponential decay $\exp(-2\hbar t/\Gamma_i)$, where Γ_i is the width of the corresponding Lorentzian.

Fig. 3 shows the normalized intermediate scattering function $S(\mathbf{Q}, t)$ for Ni diffusion in NiGa as measured at the spin–echo spectrometer SPAN at BENSC and as calculated for different values of β, where $\beta = \tau_{Ga}/\tau_{Ni}$ denotes the ratio of the mean residence times of an Ni atom on the Ga and the Ni sublattice, respectively. In this way, β can be obtained from a single spectrum with good accuracy. For the present case a value of $\beta = 0.14$ was found, in perfect agreement with results from backscattering spectrometers.

3. Diffusion studies with NRS

Nuclear resonant scattering of synchrotron radiation (NRS) (Gerdau *et al.*, 1985) measures the loss of coherence of forward-scattered radiation which is caused by the motion of diffusing atoms. Usually, one uses the Mössbauer isotope ^{57}Fe, to which we will refer in the following.
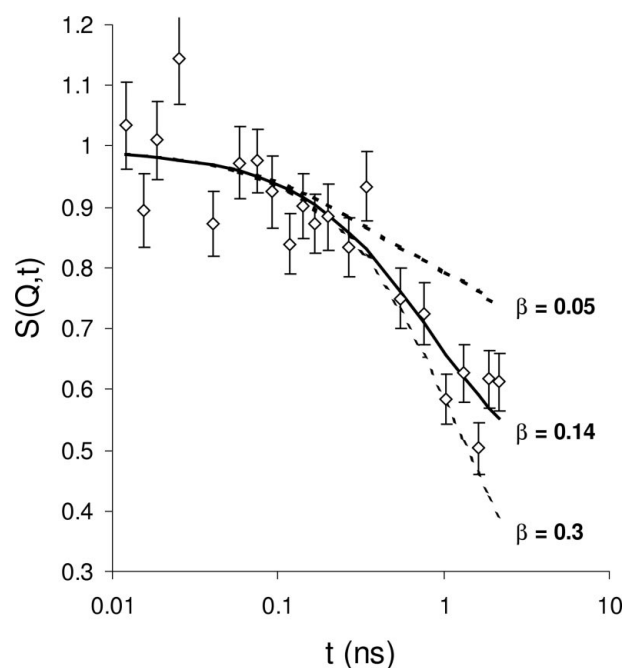

Figure 2
Quasielastic spectrum for a $Co_{64}Ga_{36}$ single crystal at $Q = 1.78\,\text{Å}^{-1}$ (Kaisermayr, Combet, Ipser *et al.*, 2001). Measurements were performed at 1403 K. The solid line represents the resolution function. Inset: Q-dependence of the linewidth of the narrow line as calculated (line) and fitted to the experimental spectra (points) for the same sample, temperature and orientation.

Figure 3
Intermediate scattering function as measured on an $Ni_{52.5}Ga_{47.5}$ single crystal at 1373 K and $2\Theta = 130°$ (Kaisermayr, Pappas *et al.*, 2001). The lines represent the intermediate scattering functions as calculated for $D_{Ni} = 3.5 \times 10^{-12}\,\text{m}^2\,\text{s}^{-1}$ on the basis of NN jumps with different ratios of residence times $\beta = \tau_{Ga}/\tau_{Ni}$.

In contrast to neutron scattering, the resonant scattering process at an ^{57}Fe nucleus is subdivided into two distinct temporary separated parts: the absorption of the photon of a short X-ray pulse (typical pulse length ~100 ps), and, on the other hand, the re-emission with a lifetime of 141 ns. Since the absorption process is well defined in time for all nuclei, the re-emission happens coherently in the forward direction (and, for some orientations of a single crystalline sample, in Bragg directions). This, however, requires that the re-emitting atoms occupy *exactly* the same positions they occupied when excited by the X-ray pulse. An atom that changes its position after the excitation by the pulse will immediately lose the proper phase with respect to the waves emitted by the other atoms (Fig. 4). Hence, the corresponding intensity will be scattered isotropically and a loss of intensity emitted in the forward direction will be observed. Since the number of misplaced atoms increases with the time after the pulse, a time-dependent decay can be observed. This decay is proportional to the square of the intermediate scattering function (Smirnov & Kohn, 1995).

3.1. Forward scattering

The first NRS experiment on diffusion was performed on Fe$_3$Si (Sepiol *et al.*, 1996). Fig. 5 shows the time-dependent decay of forward-scattered resonant intensity for various temperatures as measured on Fe in Fe$_3$Si. It is clearly visible that the increasing diffusion coefficient leads to an accelerated decay of the intensity scattered in the forward direction (which corresponds to an increasing intensity scattered into 4π).

Since the accessible time interval, and therewith the observable residence times, corresponds to some 100 ns, this method represents an ideal probe for diffusivities of the order of 10^{-14} m^2. The high brilliance and low divergence of the synchrotron beam enables short measurements with high angular resolution.

The superiority of NRS over QNS in terms of particle flux is less pronounced than one might expect. This is due to the fact that only a very small proportion (roughly one photon out of 10^9) of the incident radiation with an energy around 14.4 keV has the appropriate energy for resonant scattering. This proportion is considerably higher for QNS where a μeV energy band is selected of the incoming cold neutrons with energies in the meV range. The same holds for NSE where the flux does not scale with the energy resolution.

Fig. 6 shows how the time-integrated intensity changes with the variation of the angle between the wavevector **Q** and the crystal axes, which is obtained by rotating an FeAl single crystal in the beam (Sepiol, Czihak *et al.*, 1998). Every point in Fig. 6 corresponds to an
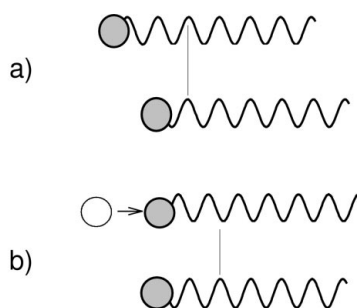
integration over all time channels of a spectrum comparable with those shown in Fig. 5. This time-integrated intensity is then directly related to the decay rates.
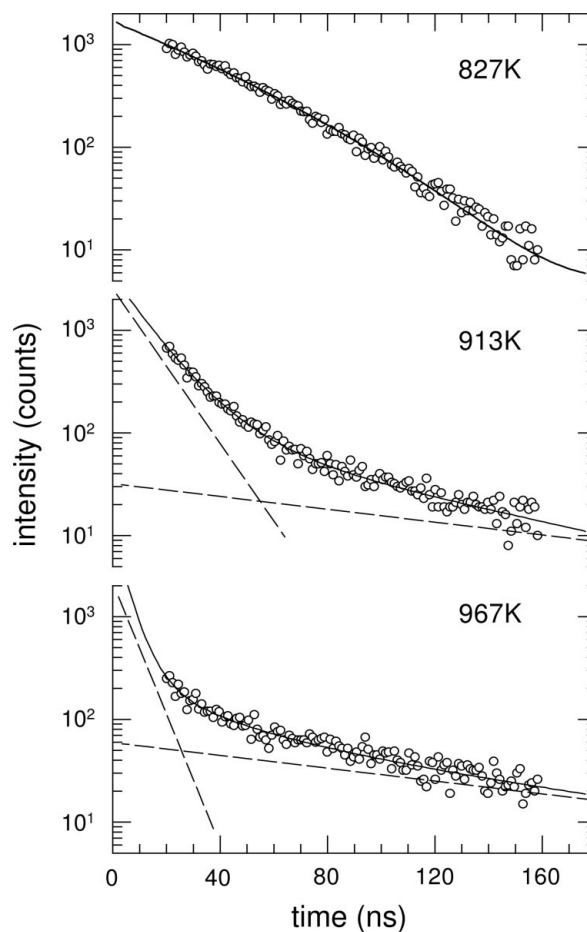

Figure 5
Time-dependence of the intensity scattered from an Fe$_3$Si single crystal into the forward direction as a function of time at three temperatures (Sepiol, Meyer *et al.*, 1998).
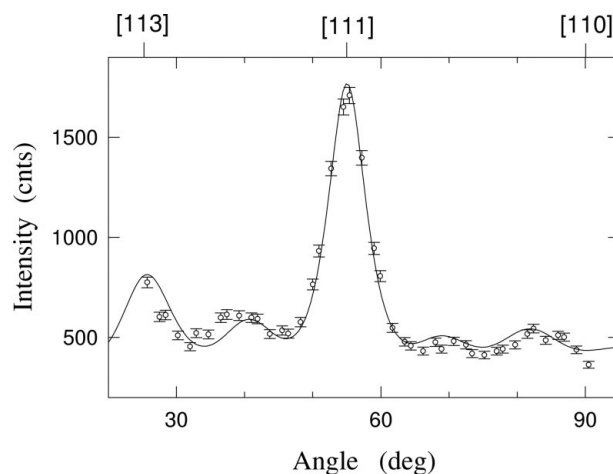

Figure 6
Time-integrated intensity of the resonantly scattered signal from an FeAl single crystal for various scattering angles (Sepiol, Meyer *et al.*, 1998). High values correspond to low decay rates. The solid line represents a fit with a nearest-neighbour jumps model. This model assumes that two subsequent jumps are preferably combined into an effective jump in the $\langle 110 \rangle$ direction.

Figure 4
Instantly after the excitation by the X-ray pulse all ^{57}Fe nuclei re-emit in phase in the forward direction (*a*). A jump of an individual atom during a time interval after the pulse that is comparable with the ^{57}Fe lifetime of 141 ns leads to a dephasing (*b*).

FeAl exhibits a *B*2 structure, similar to NiGa and CoGa. Indeed, the NRS measurements show that Fe atoms use the same jump, *i.e.* an NN jump, as Ni atoms in NiGa and Co atoms in CoGa, despite the considerable differences in the ordering energies in these alloys. However, in contrast to NiGa and CoGa, the atoms seem to prefer a combination of subsequent jumps which leads them along the ⟨110⟩ direction of the *B*2 unit cell. This might be attributed to the considerably lower vacancy concentration in this alloy and differences in atom–vacancy interactions (Sepiol *et al.*, 2001). Monte Carlo simulations show that this phenomenon can be attributed to a correlated motion where some sequences are preferred over others due to different atom–vacancy configurations (Weinkamer *et al.*, 1999). The scattering model has to take into account the successive scattering *via* the nuclear forward and nuclear Bragg diffracting channels.

3.2. Bragg scattering

NRS in forward directions requires necessarily a transmission geometry. While this set-up is convenient in most cases, some alloys cannot be prepared as sufficiently thin slices (10–100 μm) owing to their brittleness. These compounds are advantageously studied in Bragg-scattering geometry.

For perfect single crystals the theoretical description would be rather straightforward. However, relevant crystals normally exhibit a considerable mosaic spread which demands for an extended theoretical description (Thiess *et al.*, 2001). The scattering model has to take into account the successive scattering *via* the nuclear forward and nuclear Bragg diffracting channels.

3.3. Grazing incidence

A first application of NRS to surface diffusion was the near-surface diffusion of iron in iron (Sladecek *et al.*, 2002). An epitaxially grown ^{57}Fe layer was positioned at an angle of 2 mrad relative to the synchrotron beam. This corresponds to a penetration depth of about 40 Å. A typical spectrum is shown in Fig. 7. Experiments on ^{57}Fe monolayers are currently underway.

3.4. Time-domain interferometry

Time-domain interferometry of synchrotron radiation was initially applied to diffusion in amorphous materials (Baron *et al.*, 1997). In principle, this technique allows diffusion studies in an unlimited number of intermetallic alloys. However, the quasielastic effects can only be observed on diffuse scattering owing to lattice disorder (Kaisermayr, Sepiol *et al.*, 2001). Since, in ordered alloys, this corresponds to very low intensities, even third-generation synchrotrons cannot provide the brilliance necessary to apply this method to self-diffusion in metals. This situation is expected to change with the upcoming of new sources like the free-electron laser.

4. Synergies and specific advantages

Both methods, QNS and NRS, determine the scattering functions which are linked to the self-correlation function of the diffusing atoms *via* one (measurement in the time domain) or two (measurement in energy domain) Fourier transformations. Thus, both techniques provide information on the lengths, directions and frequencies of atomic jumps. Since they rely on different scattering processes they probe diffusion in different dynamical and spatial ranges.

4.1. Accessible dynamical ranges

QNS at backscattering spectrometers allows one to resolve diffusion down to 10^{-12} m^2 s^{-1}, *i.e.* at least one jump every nanosecond on average is required for this method. In this respect, QNS is ideal for diffusion studies at high temperatures, often close to the melting point (*e.g.* see Kaisermayr *et al.*, 2000; Kaisermayr, Combet, Ipser *et al.*, 2001). NRS, on the other hand, probes diffusion around $D = 10^{-14}$ m^2 s^{-1}, where mean residence times are of the order of 100 ns (see Fig. 8). This enables studies either at temperatures well below the melting point or in systems with fewer defects and hence slower diffusion. NSE spectroscopy is expected to close the gap between backscattering-QNS and NRS, since this technique allows diffusion to be observed on the 10 ns scale.
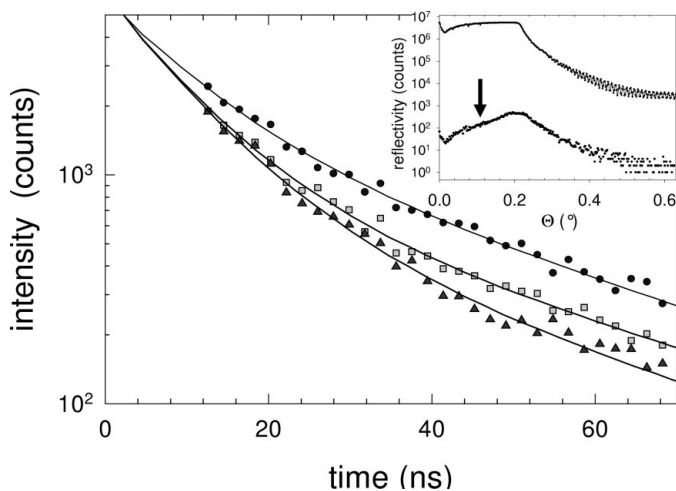

Figure 7
Time-dependence of the resonant signal from Fe/MgO(100) in grazing-incidence geometry at 1090 K (circles), 1200 K (squares) and 1230 K (triangles). Inset: angular dependence of the time-integrated intensity of resonant scattering on the ^{57}Fe nuclei (lower curve) and electronic scattering on the atomic shell (upper curve) for the same sample.
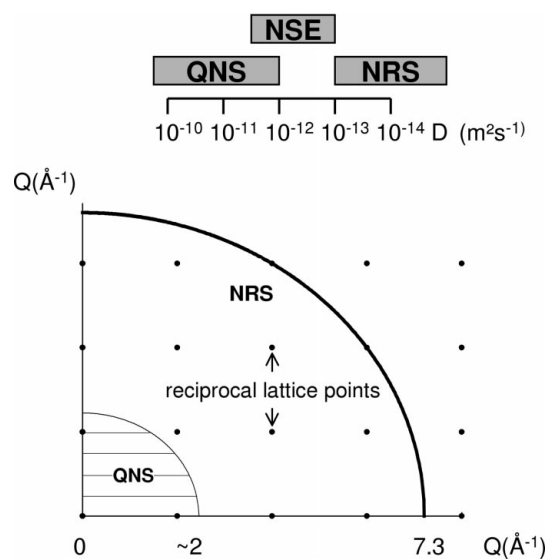

Figure 8
Top: dynamical ranges (diffusivities) accessible with QNS on backscattering spectrometers, NSE and NRS. Bottom: *Q* ranges accessible with QNS (including NSE) and NRS with ^{57}Fe. The reciprocal lattice points correspond to a simple cubic lattice with a lattice spacing of about 3.1 Å.

Table 1
Comparison between quasielastic neutron scattering (QNS) and nuclear resonant scattering (NRS) for self-diffusion in metals.

Method	QNS, NSE	NRS
Q range	0–2 Å^{-1}	7.3 Å^{-1}
Energy resolution	$\sim$0.1 µeV	neV
Diffusivities	$\geq$10^{-13} m^2 s^{-1}	$\sim$10^{-14} m^2 s^{-1}
Dynamical range	< 10 ns	10–10^3 ns
Probe atoms	Ni, Co, V, Ti . . .	^{57}Fe
Long-range diffusion	Yes	No

4.2. Spatial resolution

Fig. 8 shows that while the scattering vector for NRS is inherently limited to 7.3 Å^{-1} (constant momentum of the ^{57}Fe Mössbauer photon), it is possible to probe a Q range of about 0.1–2 Å^{-1} with QNS. This means that both methods are able to resolve diffusion processes on the angstrom scale. Additionally, QNS also yields information on long-range diffusivities, when measurements are carried out at $Q < 0.5$ Å^{-1}. Hence, QNS allows one to compare jump frequencies with macroscopic diffusion and, thus, to determine the degree of correlation of subsequent jumps. In principle this can also be achieved with NRS by comparing jump frequencies with long-range diffusivities from radio tracer measurements. However, since QNS allows one to obtain the information on diffusion on both scales simultaneously (hence at exactly the same temperature and composition), neutron scattering allows correlation factors to be determined with higher accuracy. On the other hand, the highly parallel synchrotron beam leads to an excellent Q-resolution of NRS.

4.3. Accessible samples

QNS requires samples that contain strong incoherent scatterers like, *e.g.* Ni, Co, V or Ti. NRS, on the other hand, is practically limited† to one single isotope, ^{57}Fe.

There are several basic intermetallic structures where diffusion has been investigated in different alloys with the two methods. Therewith, it was possible to determine to which extent the – sometimes enormous – differences in the diffusion rate or defect structure of related systems are connected to the microscopic diffusion mechanism. Examples of investigated systems are: the cubic *B*2 structure [FeAl (Sepiol, Czihak *et al.*, 1998) with NRS; NiGa (Kaisermayr *et al.*, 2000), CoGa (Kaisermayr, Combet, Ipser *et al.*, 2001) with QNS], the cubic *D*0$_3$ structure [Fe$_3$Si (Sepiol *et al.*, 1996) with NRS; Ni$_3$Sb (Vogl *et al.*, 1996) with QNS], the hexagonal *B*8 structure [FeSb (Sladecek *et al.*, 2001) with NRS; NiSb (Vogl *et al.*, 1993) with QNS]. Hence, the complementarity of NRS and QNS regarding the observable elements allows not only the determination of diffusion in single alloys but to obtain a picture of diffusion in whole classes of alloys. For an overview of the specific features of QNS and NRS, see Table 1.

5. Conclusion

Quasielastic neutron scattering and nuclear resonant scattering of synchrotron radiation allow one to observe the lengths, directions and frequencies of atomic jumps. Since the two methods monitor different dynamical ranges with different elements as probe atoms, a combination of both gives access to diffusion in whole classes of alloys where the individual representatives differ sometimes strongly in their dynamical behaviour. Thus, it is possible to determine to what extent parameters like ordering energy, composition or temperature influence diffusion.

Specific advantages of QNS are the large range of accessible samples and the possibility of measuring simultaneously the microscopic and macroscopic features of diffusion. NRS, on the other hand, provides the best energy resolution and thus gives access to slower diffusion than does QNS. In addition, this method offers an excellent momentum resolution.

References

Baron, A. Q. R., Franz, H., Meyer, A., Rüffer, R., Chumakov, A. I., Burkel, E. & Petry, W. (1997). *Phys. Rev. Lett.* **79**, 2823–2826.
Cook, J. C., Richter, D., Benham, M. J., Ross, D. K., Hempelmann, R., Anderson, I. S. & Sinha, S. K. (1990). *J. Phys. Condens. Matter*, **2**, 79–94.
Gerdau, E., Rüffer, R., Winkler, H., Tolksdorf, W., Klages, C. & Hannon, J. (1985). *Phys. Rev. Lett.* **54**, 835–838.
Hempelmann, R. (2000). *Quasielastic Neutron Scattering and Solid State Diffusion.* Oxford: Clarendon Press.
Kaisermayr, M., Combet, J., Ipser, H., Schicketanz, B., Sepiol, B. & Vogl, G. (2000). *Phys. Rev. B*, **61**, 12038–12044.
Kaisermayr, M., Combet, J., Ipser, H., Schicketanz, B., Sepiol, B. & Vogl, G. (2001). *Phys. Rev. B*, **63**, 054303-1–054303-8.
Kaisermayr, M., Combet, J., Sepiol, B. & Vogl, G. (2001). *Defect Diffus. Forum*, **194/199**, 461–466.
Kaisermayr, M., Pappas, C., Sepiol, B. & Vogl, G. (2001). *Phys. Rev. Lett.* **87**, 175901-1–175901-4.
Kaisermayr, M., Sepiol, B., Thiess, H., Vogl, G., Alp., E. E. & Sturhahn, W. (2001). *Eur. Phys. J.* **20**, 335–341.
Kaisermayr, M., Sepiol, B. & Vogl, G. (2001). *Physica B*, **301**, 115–118.
Kutner, R. & Sosnowska, I. (1977). *J. Phys. Chem. Solids*, **38**, 741–746.
Mehrer, H. (1996). *Mater. Trans. Jap. Inst. Met.* **37**, 1259–1280.
Randl, O. G., Sepiol, B., Vogl, G., Feldwisch, R. & Schroeder, K. (1994). *Phys. Rev. B*, **49**, 8768–8773.
Rowe, J. M., Sköld, K., Flotow, H. E. & Rush, J. J. (1971). *J. Phys. Chem. Solids*, **32**, 41–54.
Sepiol, B., Czihak, C., Meyer, A., Vogl, G., Metge, J. & Rüffer, R. (1998). *Hyperfine Interact.* **113**, 449–454.
Sepiol, B., Löser, W., Kaisermayr, M., Weinkamer, R., Fratzl, P., Thiess, H., Sladecek, M. & Vogl, G. (2001). *Defect Diffus. Forum*, **194/199**, 349–356.
Sepiol, B., Meyer, A., Vogl, G., Franz, H. & Rüffer, R. (1998). *Phys. Rev. B*, **57**, 10433–10439.
Sepiol, B., Meyer, A., Vogl, G., Rüffer, R., Chumakov, A. I. & Baron, A. Q. R. (1996). *Phys. Rev. Lett.* **76**, 3220–3223.
Sladecek, M., Miglierini, M., Sepiol, B., Ipser, H., Schicketanz, H. & Vogl, G. (2001). *Defect Diffus. Forum*, **194/199**, 369–374.
Sladecek, M., Sepiol, B., Kaisermayr, M., Korecki, J., Handke, B., Thiess, H., Leupold, O., Rüffer, R. & Vogl, G. (2002). *Surface Sci.* C**507/510**, 124–128.
Smirnov, G. V. & Kohn, V. G. (1995). *Phys. Rev. B*, **52**, 3356–3365.
Thiess, H. (2001). PhD thesis, Universität Wien, Vienna, Austria.
Thiess, H., Kaisermayr, M., Sepiol, B., Sladecek, M., Rüffer, R. & Vogl, G. (2001). *Phys. Rev. B*, **64**, 104305-1–104305-10.
Vogl, G. & Feldwisch, R. (1998). *Diffusion in Condensed Matter*, edited by J. Kärger, P. Heitjas & R. Haberlandt, p. 40. Vieweg, Braunschweig/ Wiesbaden.
Vogl, G., Kaisermayr, M. & Randl, O. G. (1996). *J. Phys. Condens. Matter*, **8**, 4727–4738.
Vogl, G., Randl, O. G., Petry, W. & Hünecke, J. (1993). *J. Phys. Condens. Matter*, **5**, 7215–7230.
Weinkamer, R., Fratzl, P., Sepiol, B. & Vogl, G. (1999). *Phys. Rev. B*, **59**, 8622–8625.

---

† There are several other Mössbauer isotopes which can be excited with synchrotron undulator sources, but they all suffer from a more or less short lifetime. An NRS feasibility experiment on ^{119}Sn diffusion is reported by Thiess (2001).